EOS Aura Science Team Meeting
30 August – 1 September, 2016 | Rotterdam, The Netherlands

Hydrological controls on the tropospheric ozone greenhouse gas effect

Le (Elva) Kuai[1], Kevin W. Bowman[2], Helen Worden[3], Robert L. Herman[2], Susan S. Kulawik[4]

1. JIFRESSE/UCLA;
2. JPL/Caltech;
3. NCAR;
4. BAER Institute/NASA Ames;

Objectives and Motivations

Tropospheric Emission Spectrometer (TES)

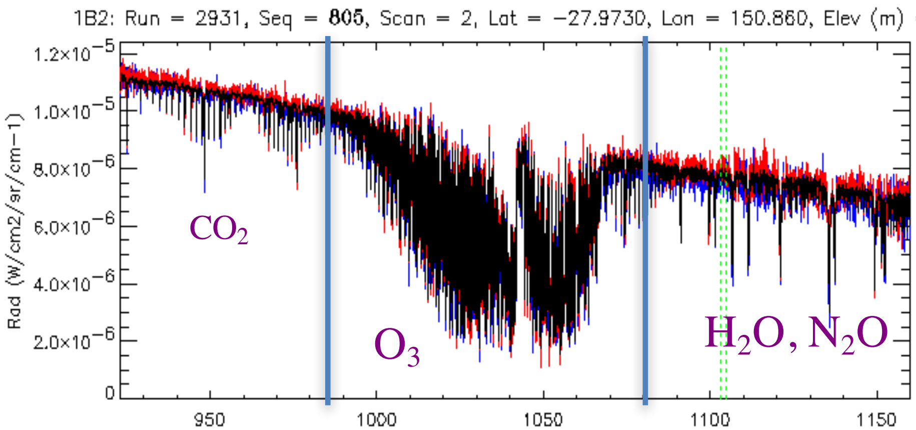

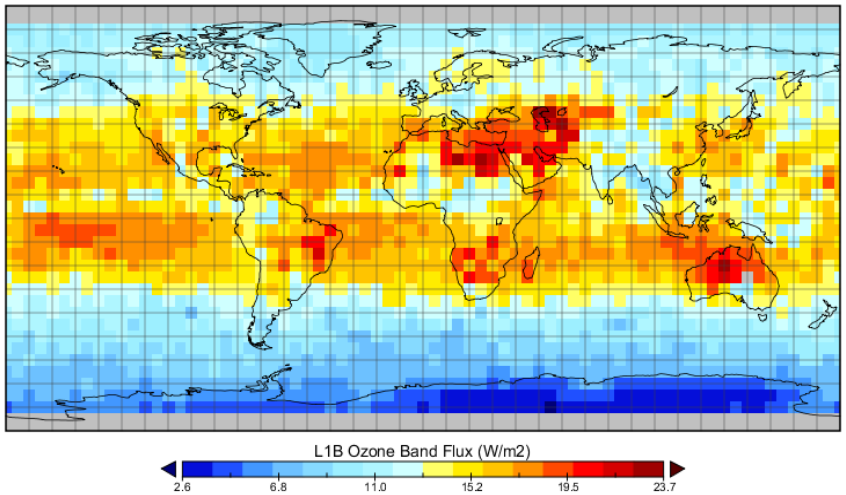

- Attribute the **TOA flux change** due to dominant physical quantities.

$$\underbrace{\Delta F_{TOA}}_{\text{9.6 µm band flux change}} = \underbrace{\frac{\partial F_{TOA}}{\partial O_3}\Delta O_3}_{O_3} + \underbrace{\frac{\partial F_{TOA}}{\partial T_{sur}}\Delta T_{sur}}_{\text{Surface temperature}} + \underbrace{\frac{\partial F_{TOA}}{\partial T_{atm}}\Delta T_{atm}}_{\text{Atmos. temperature}} + \underbrace{\frac{\partial F_{TOA}}{\partial H_2O}\Delta H_2O}_{\text{Water vapor}} + \underbrace{\frac{\partial F_{TOA}}{\partial \tau_{cloud}}\Delta \tau_{cloud}}_{\text{Cloud}} + \underbrace{r_s}_{\text{residual}}$$

Instantaneous Radiative Kernels (IRK): $\mathrm{IRK}_{O_3}(z) = \dfrac{\partial F_{TOA}(q)}{\partial O_3(z)}$

Objectives and Motivations

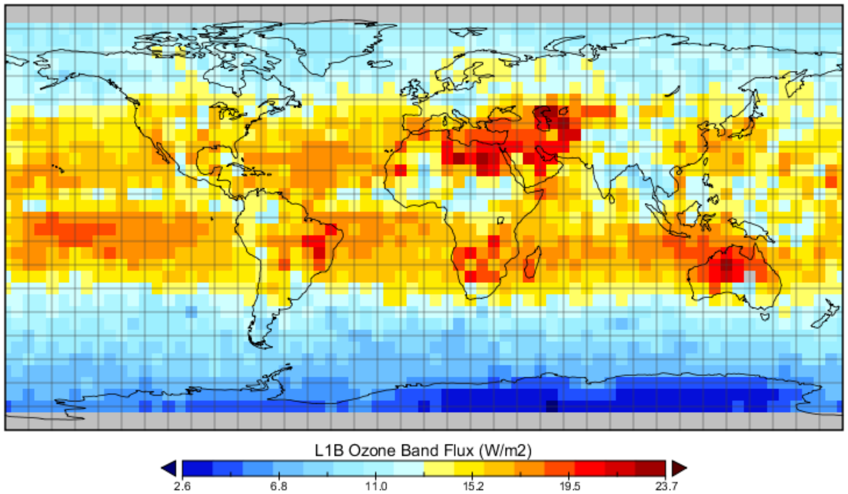

- Attribute the **TOA flux change** due to dominant physical quantities.

- Understand the dependence of O_3 IRK variation on **H_2O, temperature, and clouds.**

Tropospheric O3
GHG effect

Hydrological Cycle

$$\underbrace{\Delta F_{TOA}}_{\text{9.6 µm band flux change}} = \underbrace{\frac{\partial F_{TOA}}{\partial O_3}\Delta O_3}_{O_3} + \underbrace{\frac{\partial F_{TOA}}{\partial T_{sur}}\Delta T_{sur}}_{\text{Surface temperature}} + \underbrace{\frac{\partial F_{TOA}}{\partial T_{atm}}\Delta T_{atm}}_{\text{Atmos. temperature}} + \underbrace{\frac{\partial F_{TOA}}{\partial H_2O}\Delta H_2O}_{\text{Water vapor}} + \underbrace{\frac{\partial F_{TOA}}{\partial \tau_{cloud}}\Delta \tau_{cloud}}_{\text{Cloud}} + \underbrace{r_s}_{\text{residual}}$$

Instantaneous Radiative Kernels (IRK): $\mathrm{IRK}_{O_3}(z) = \dfrac{\partial F_{TOA}(q)}{\partial O_3(z)}$

Objectives and Motivations

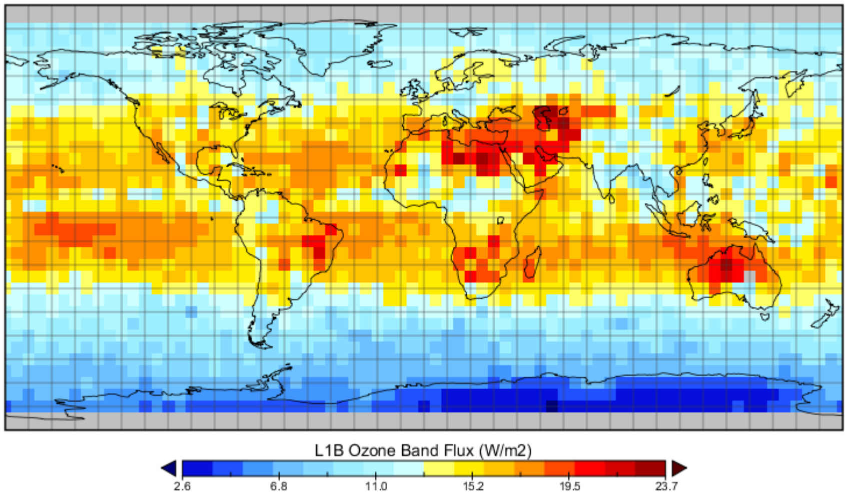

- Attribute the **TOA flux change** due to dominant physical quantities.

- Understand the dependence of O_3 IRK variation on **H_2O, temperature, and clouds.**

$$RH = \frac{e_w(H_2O,P)}{e_w^*(T,P)}$$

$$\underbrace{\Delta F_{TOA}}_{\text{9.6 µm band flux change}} = \underbrace{\frac{\partial F_{TOA}}{\partial O_3}\Delta O_3}_{O_3} + \underbrace{\frac{\partial F_{TOA}}{\partial T_{sur}}\Delta T_{sur}}_{\text{Surface temperature}} + \underbrace{\frac{\partial F_{TOA}}{\partial T_{atm}}\Delta T_{atm}}_{\text{Atmos. temperature}} + \underbrace{\frac{\partial F_{TOA}}{\partial H_2O}\Delta H_2O}_{\text{Water vapor}} + \underbrace{\frac{\partial F_{TOA}}{\partial \tau_{cloud}}\Delta \tau_{cloud}}_{\text{Cloud}} + \underbrace{r_s}_{\text{residual}}$$

Instantaneous Radiative Kernels (IRK): $\mathrm{IRK}_{O_3}(z) = \frac{\partial F_{TOA}(q)}{\partial O_3(z)}$

5-angle Gaussian Quadrature integration method

Tropospheric O_3 GHG effect

Top of atmospheric flux **(9.6μm ozone band)**:

$$F_{TOA}=\int\int_0^{2\pi}\int_0^{\frac{\pi}{2}}L_\nu(\theta)\cos\theta\sin\theta\,d\theta\,d\phi\,d\nu$$

Instantaneous Radiative Kernel **(mW/m²/ppb)**:

$$\mathrm{IRK}(z_l)=\frac{\partial F_{TOA}}{\partial q_l(z_l)}$$

Logarithm IRK **(mW/m²)**:

$$\mathrm{LIRK}(z_l)=\frac{\partial F_{TOA}}{\partial \ln q_l(z_l)}$$

Long Wave Radiative Effect (Tropospheric column) **(W/m²)**:

$$\mathrm{LWRE}=\Delta F_{TOA}=\sum_{l=surface}^{tropopause}\left(\frac{\partial F_{TOA}}{\partial q_l(z_l)}\right)q_l(z_l)$$

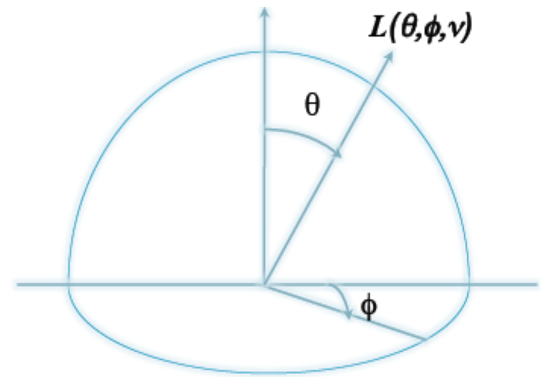

IRK | **Full Integration** | **Anisotropy**

$$\boxed{\frac{\partial F_{TOA}}{\partial q(z_l)}}=\boxed{2\pi\left[\int_{\nu_1}^{\nu_2}\int_0^{\pi/2}\frac{\partial L(\nu,\theta,\phi)}{\partial q(z_l)}\cos\theta\sin\theta\,d\theta\,d\nu\right]}\approx\boxed{2\pi\left[\sum_{i=1}^{5}w_iK(\theta^i_{\mathrm{Nadir}})\right]}$$

w_i	$\theta^i_{\mathrm{Nadir}}$ (°)
0.015748	63.6765
0.073909	59.0983
0.146387	48.1689
0.167175	32.5555
0.096782	14.5752

$$K(\theta^i_{Nadir})=\sum\left[\frac{\partial L(\nu,\theta^i_{Nadir})}{\partial q(z_l)}\right]\Delta\nu$$

$q(z_l)$ could be any atmospheric state, such as profiles of O_3, T_{atm}, H_2O, or T_{sur}, cloud OD, emissivity, etc.

[Worden et al., 2011]
[Doniki et al., 2015]

Tropospheric ozone GHG effect

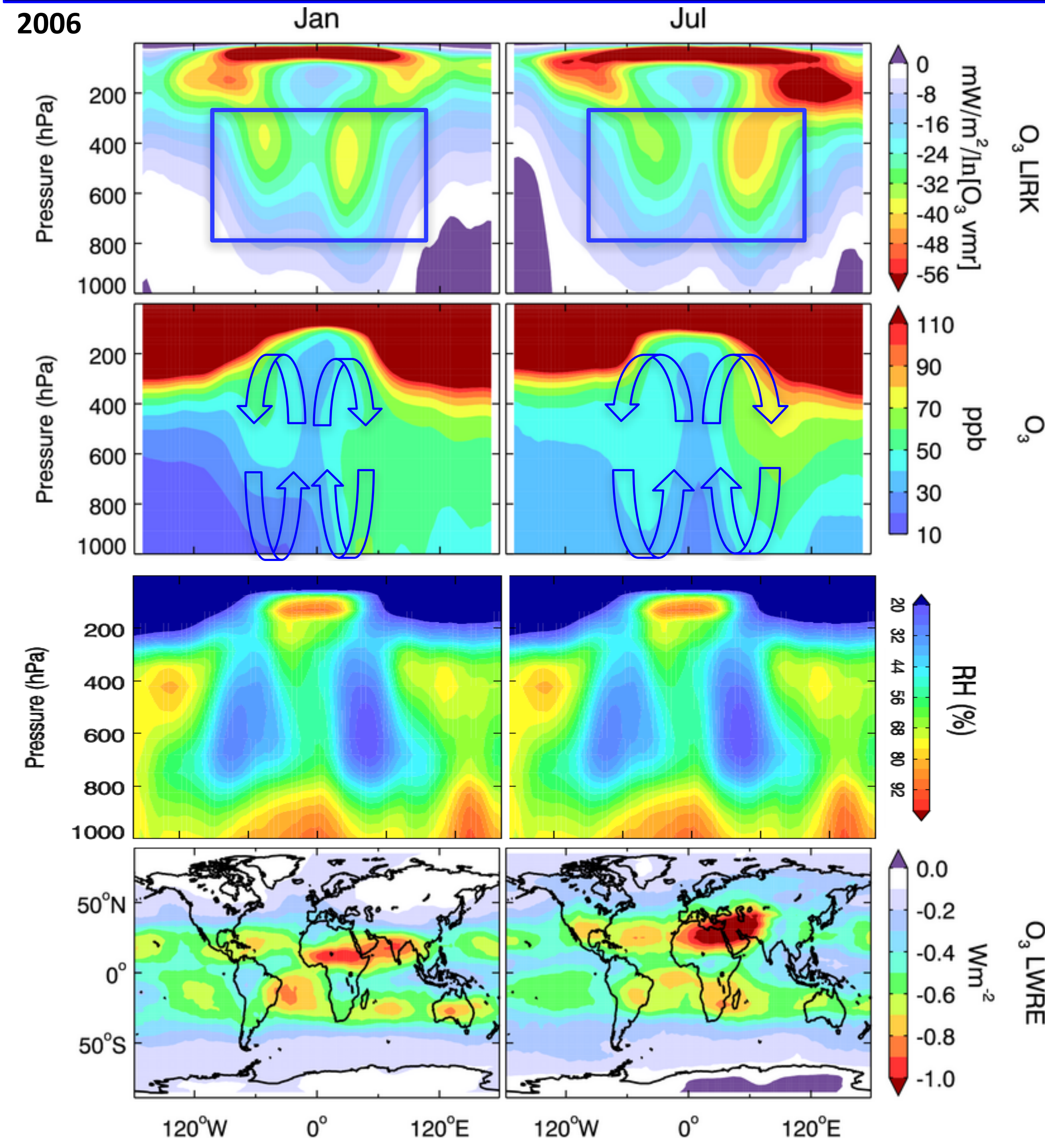

- Two secondary strong flux sensitivity in LIRK is near subtropical mid and upper troposphere in both hemispheres.
- Highest LWRE over Middle East during boreal summer (> 1 Wm^{-2}).
- Subtropical maximum and tropical low in LWRE.

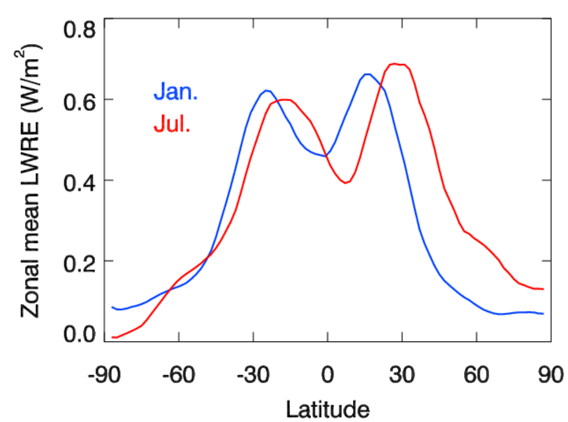

Cloud effect on ozone IRK

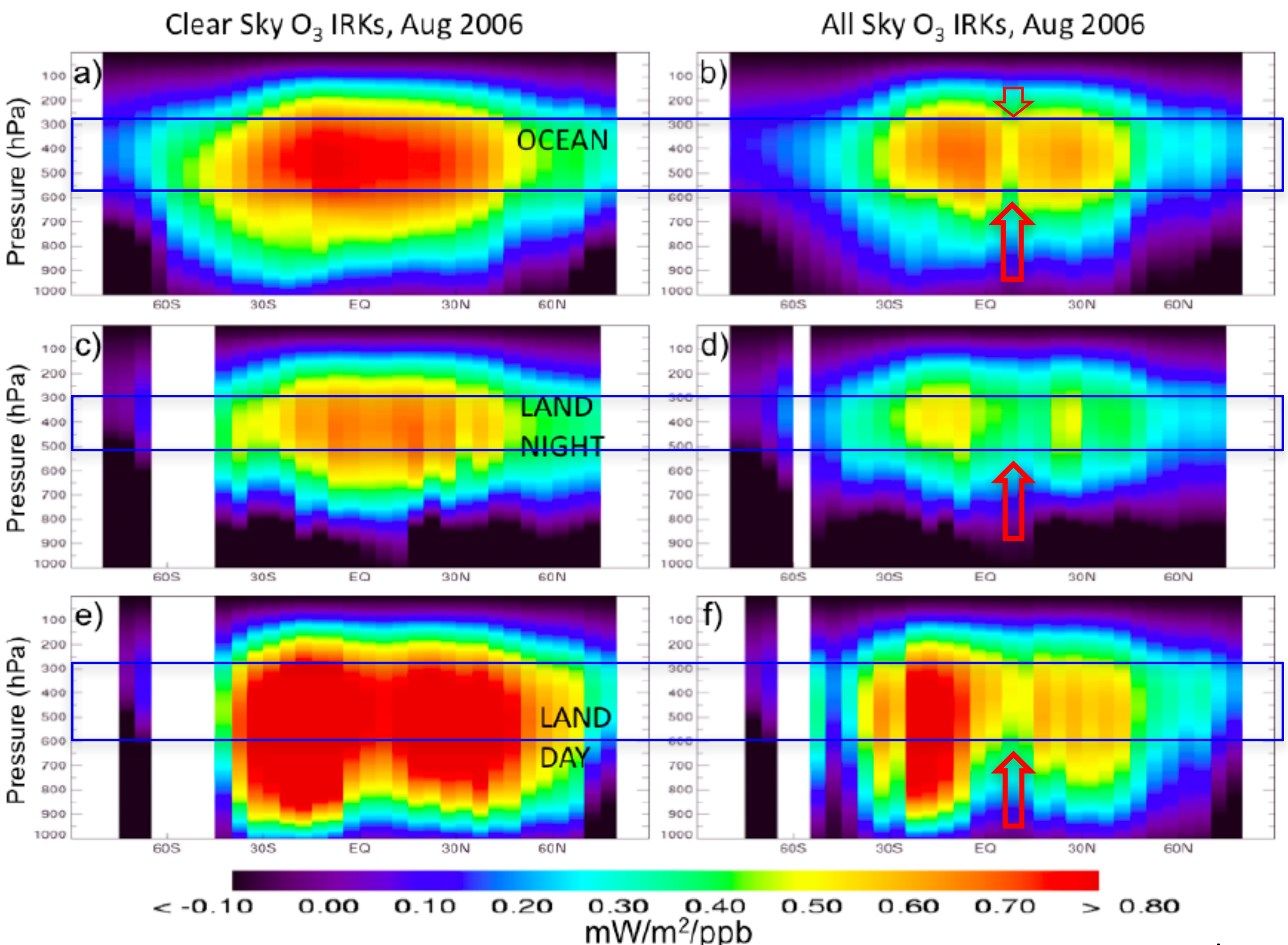

Shrink to a thinner layer shifted upwards

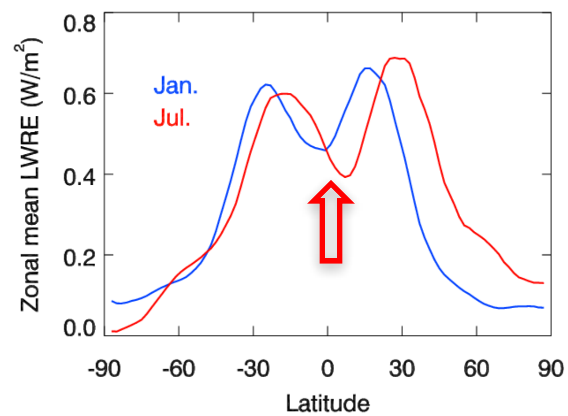

Worden et al., 2011: Fig. 3

- Clouds significantly reduce the TOA flux sensitivity to O_3 in the lower troposphere compared to the clear sky kernels (Soden et al., 2008).
- Tropical clouds also greatly reduce the mid tropospheric maximum in O_3 IRK and contribute to tropical low LWRE.

O_3 LWRE and RH

- **Similar spatial pattern in LWRE and RH**
- **Spatiotemporal change oppositely**

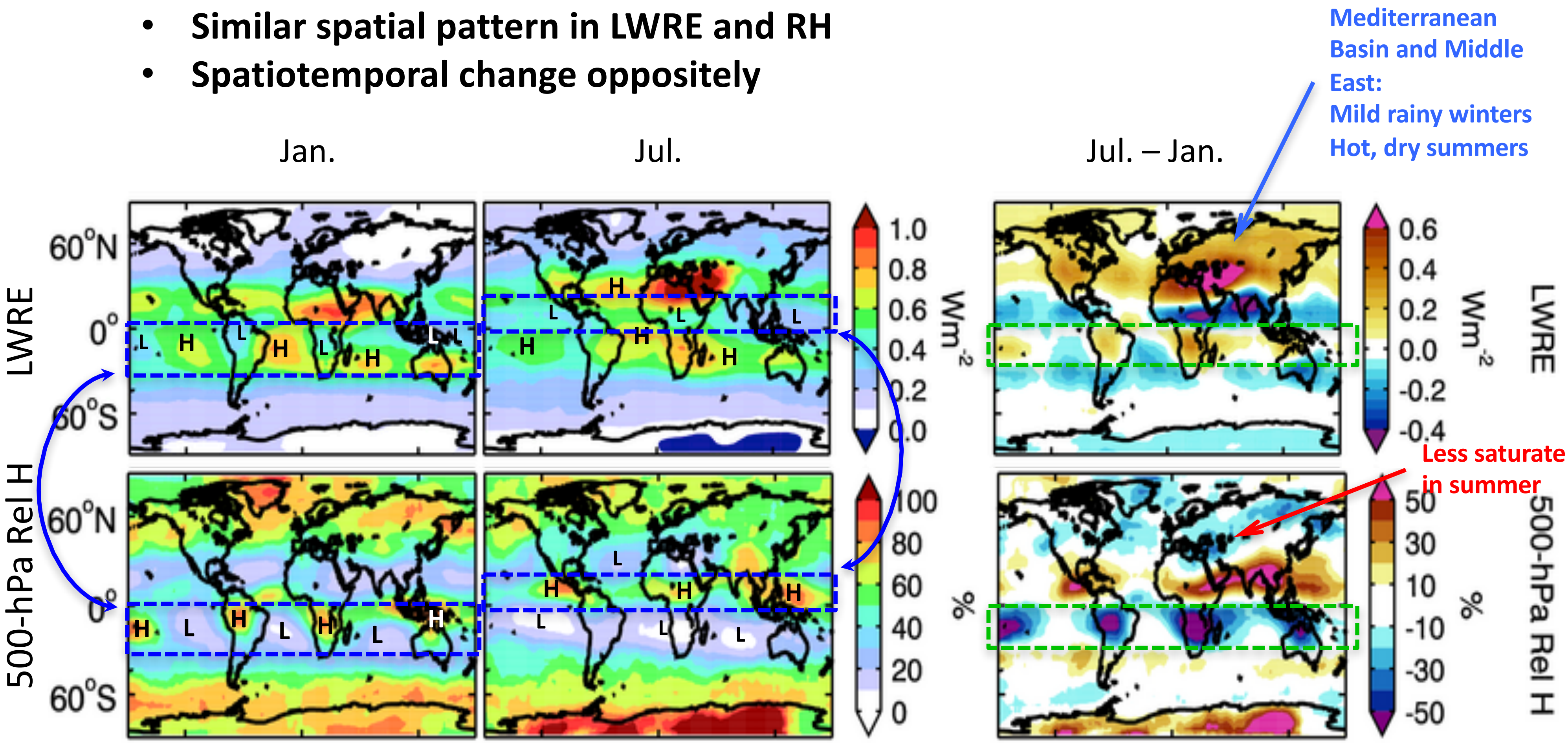

	LWRE (Wm^2)	RH (%)
High	>0.6	>80
Low	<0.4	<30

- Low LWRE within ITCZ deep convection zones.
- High LWRE over subtropical low RH regions.

O_3 LWRE and RH

- Similar spatial patter in LWRE and RH
- Spatiotemporal change oppositely

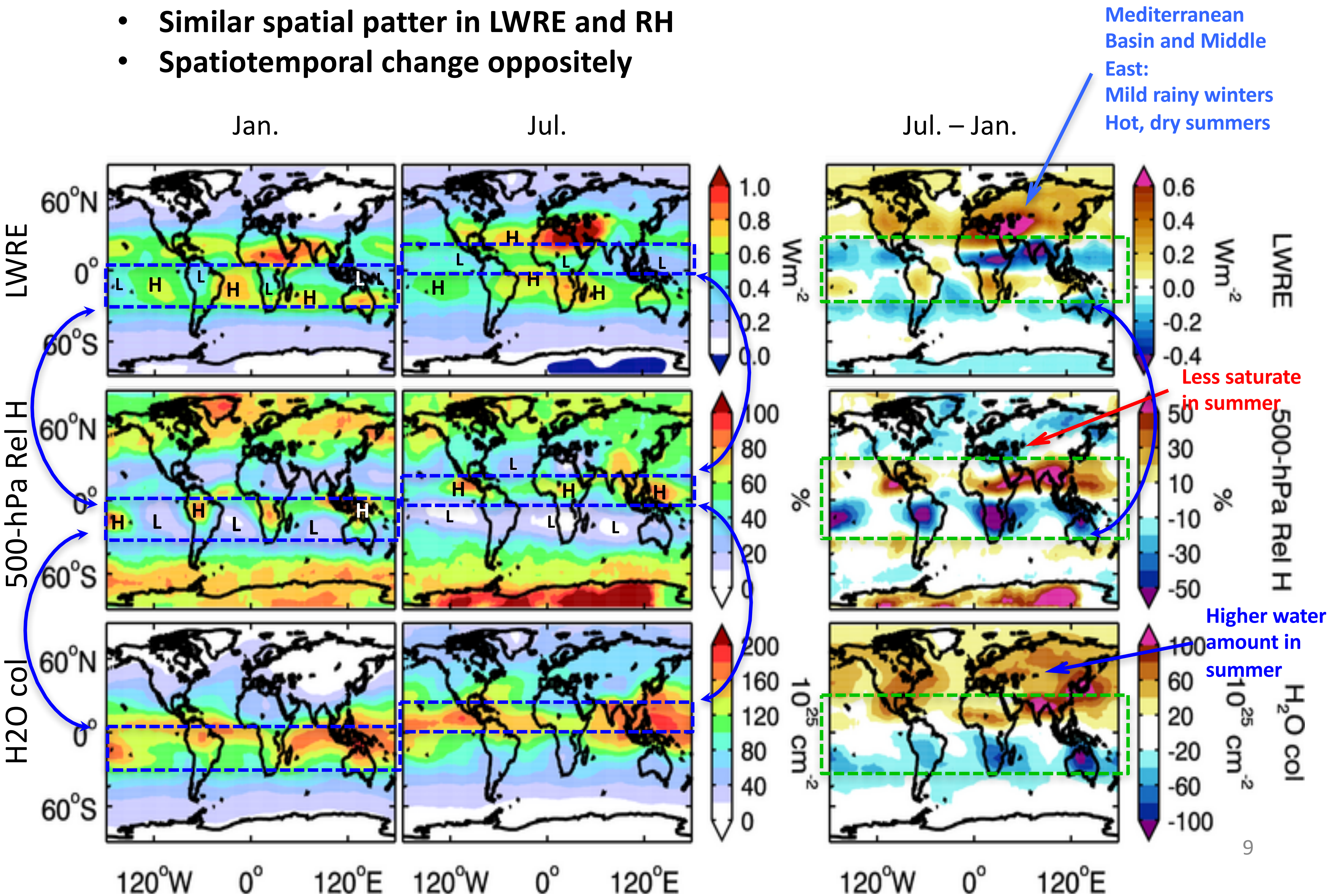

O_3 LWRE, Tropospheric O_3 column, & T_{sur}

- Australia high LWRE in Jan. is due to higher T_{sur} because large thermal contrast amplify the sensitivity
- Middle East LWRE maximum also relevant to summer O_3 enhancement (Li et al., 2001; Liu et al., 2009) and high T_{sur}.
- Africa savanna high LWRE is related to biomass burning in Jan and O_3 enhancement.
- Congo basin high LWRE in Jul. is due to O_3 enhancement.

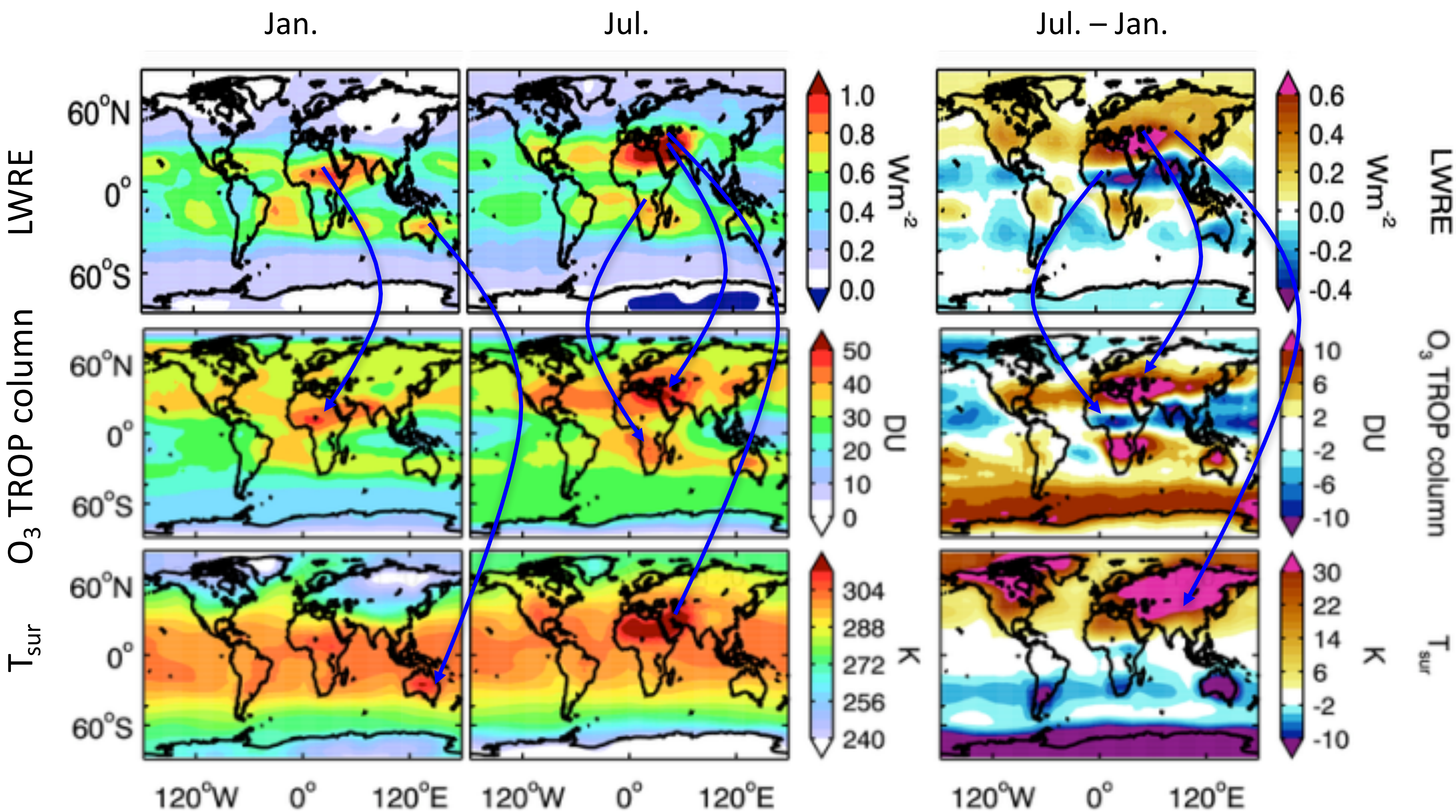

Longitude – altitude view

- ITCZ in S. Tropics | Jan.
- ITCZ in N. Tropics | Jul.

S. Tropics belt (0°~25°S)
(January)

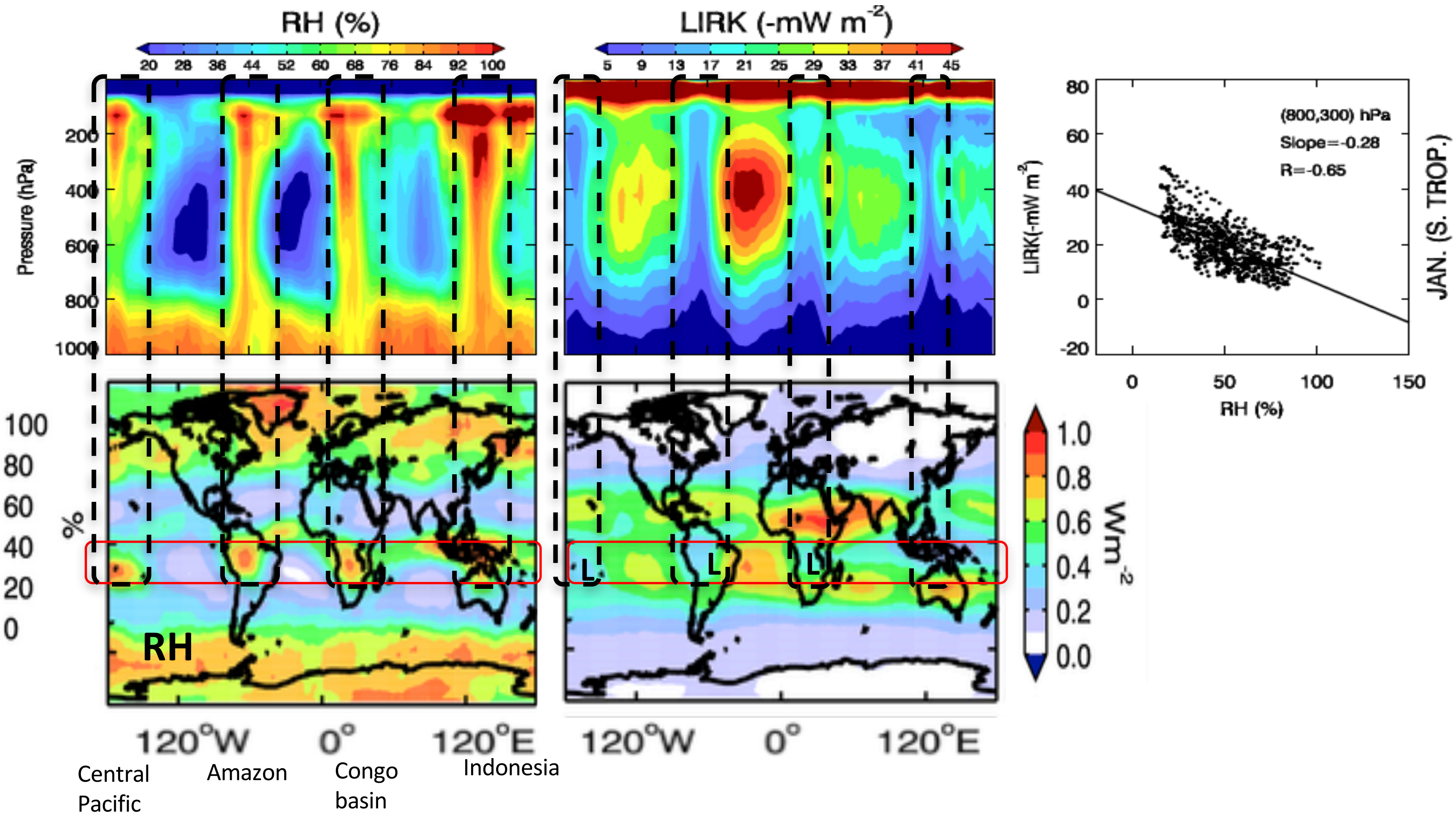

In January, at central Pacific, Amazon, Congo basin, and Indonesia, deep convection zones correspond to low ozone flux sensitivity.

The Walker circulation is the primary driver for the deep convection zones at tropical central Pacific.

Longitude – altitude view

- ITCZ in S. Tropics | Jan.
- ITCZ in N. Tropics | Jul.

N. Tropics belt (0°~5°N) (July)

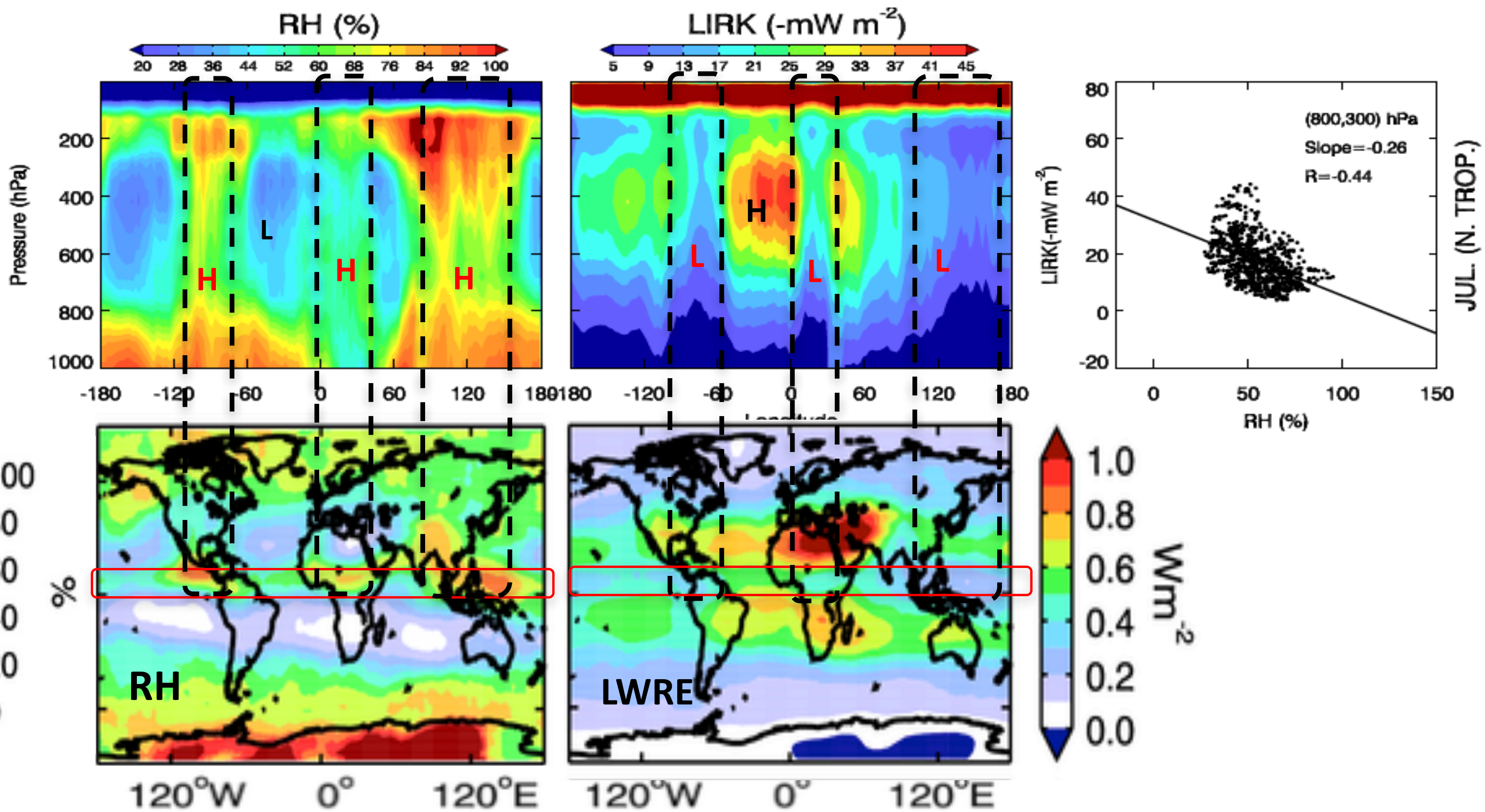

E. Tropical Pacific

Africa savanna

Southeast Asia

High RH at E. Tropical Pacific and moderate high RH at Africa savanna are another two places corresponding to low LIRK.

In July, Asian monsoon is the primary driver to bring deep convection and heavy precipitation to India and southeast Asia, where LIRK are found low.

Latitude – altitude view

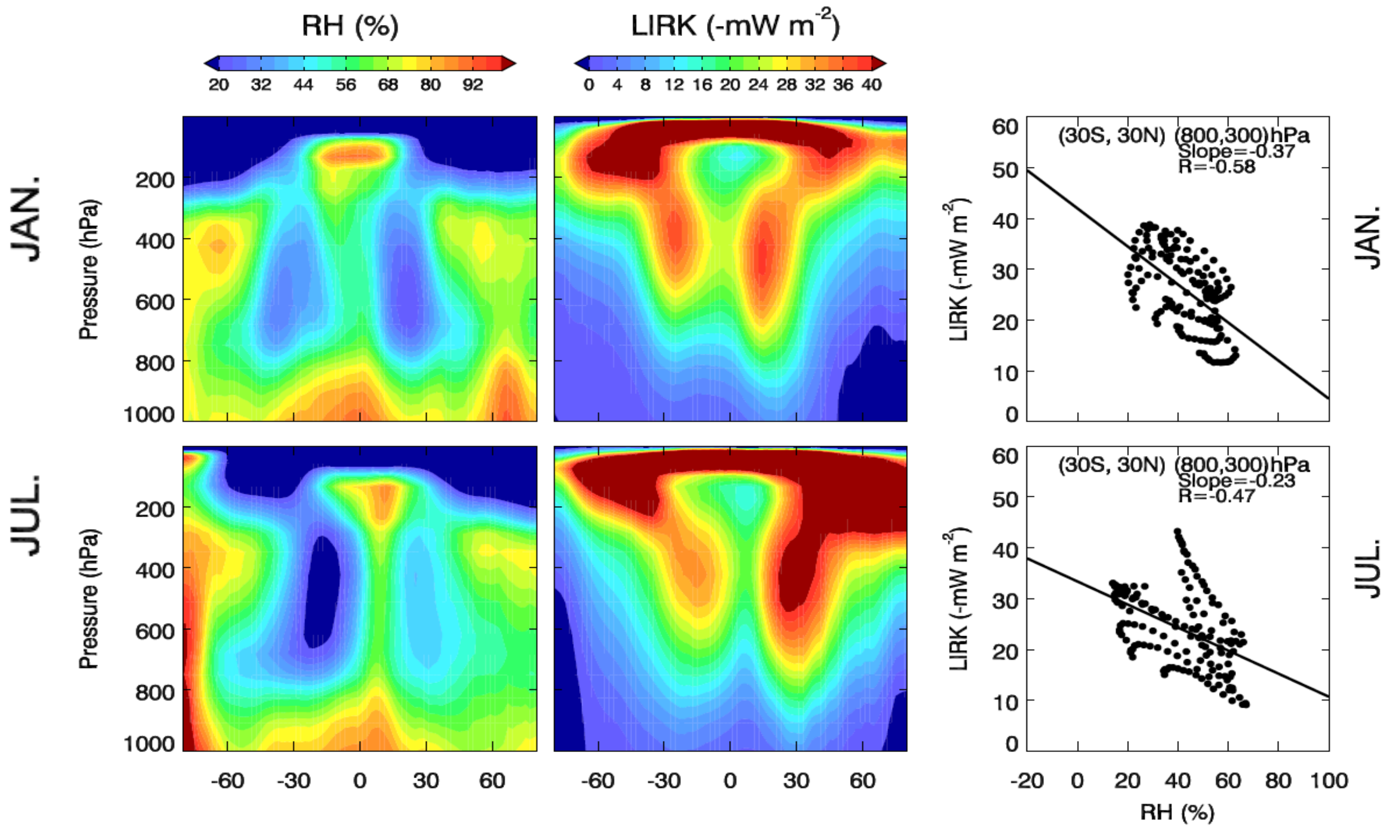

- Similar anti-correlation between RH and Ozone LIRK.
- Two mid tropospheric maximum in Ozone LIRK correspond to the subtropical arid regions where the tropopause tends to sink and the downwelling of Hadley cell dominants.

H_2O, cloud, T, O_3 signatures on O_3 GHG effect

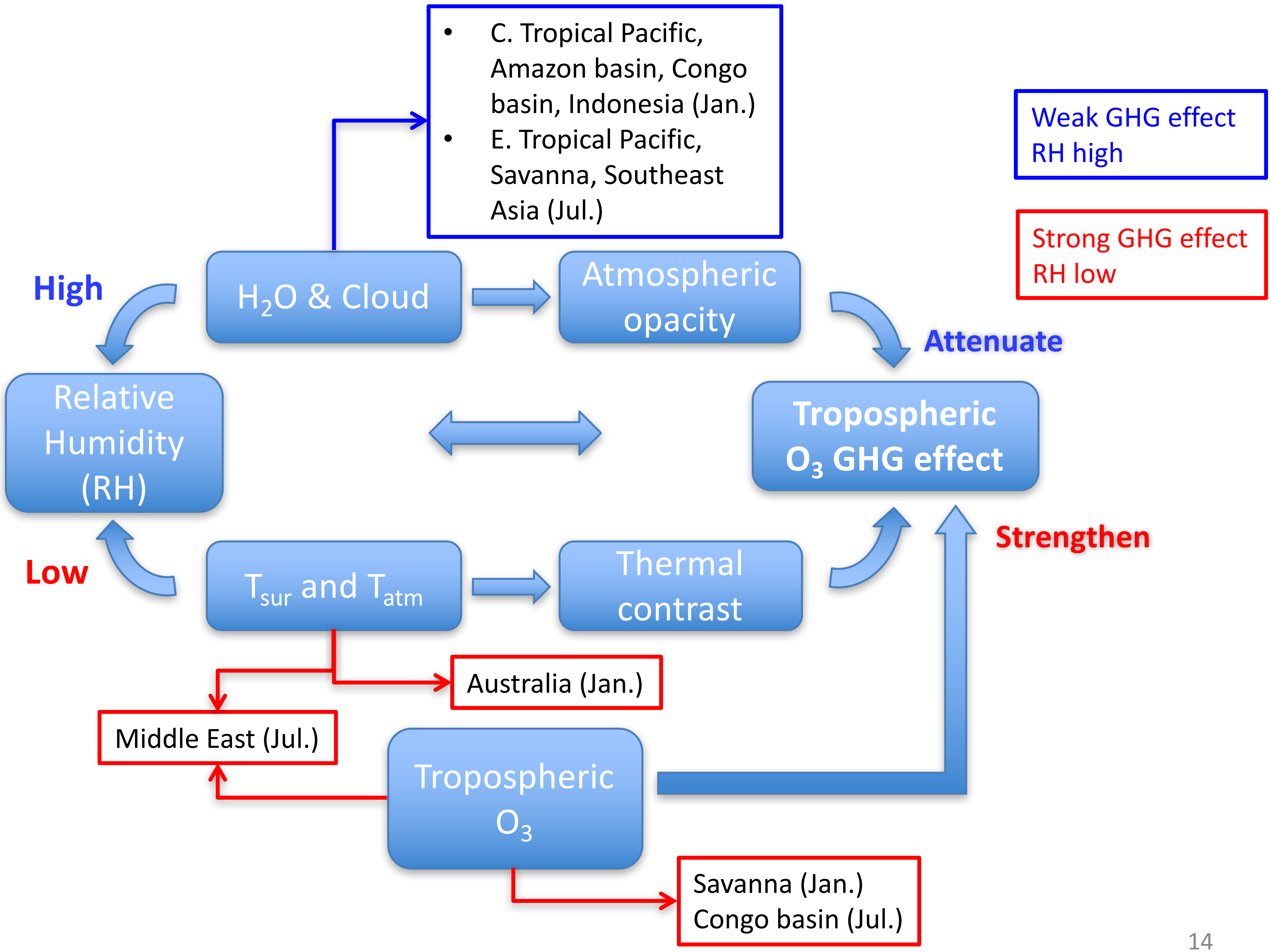

Conclusions

- The tropospheric O_3 GHG effect is low in tropics but maximized in subtropics in both hemisphere.
- RH is a useful quantity to help identify the primary driver, the large-scale circulation, that determine H_2O, temperature and cloud distribution. It also helps to understand the hydrological control on the tropospheric O_3 GHG effect.
- Tropics:
  - H_2O and clouds cause the low O_3 GHG effect.
  - The primary drivers are walker circulation and Asia summer monsoon for the deep convection.
- Subtropics:
  - Surface temperature and O_3 enhancement contribute to high O_3 GHG effect.
  - The primary drivers are the descent of tropopause height and downwelling of Hadley cell.
  - The maximum O_3 GHG effect are found at Middle East during its hot dry summer (>1 W/m^2). Ozone enhancement and high Tsur over dry desert with clear sky.

Future outlook

- **Hadley cell expansion (Seidel and Randel, 2007)**
  - The width expanding; poleward shift of the downward branch
  - Increase of global T and pole-to-equator T gradient (Frierson et al., 2007)
  - A shift in the ITCZ farther away from the equator due to the response to CO_2 forcing (Held, 2000; Kang and Lu, 2012; Lu et al., 2007)
- **Inhabitability of Middle East due to global warming (Pal et al., 2016)**
  - Additional O_3 radiative forcing to this region
- **The Asia monsoon strengthen (Li et al., 2010; Singh et al., 2014)**
  - Another positive feedback to the Middle East O_3 GHG effect

Kuai et al. 2016 submitted to ELEMENTA

Thank you !

EOS Aura Science Team Meeting

30 August – 1 September, 2016 | Rotterdam, The Netherlands

The Inter Tropical Convergence Zone (ITCZ) in RH

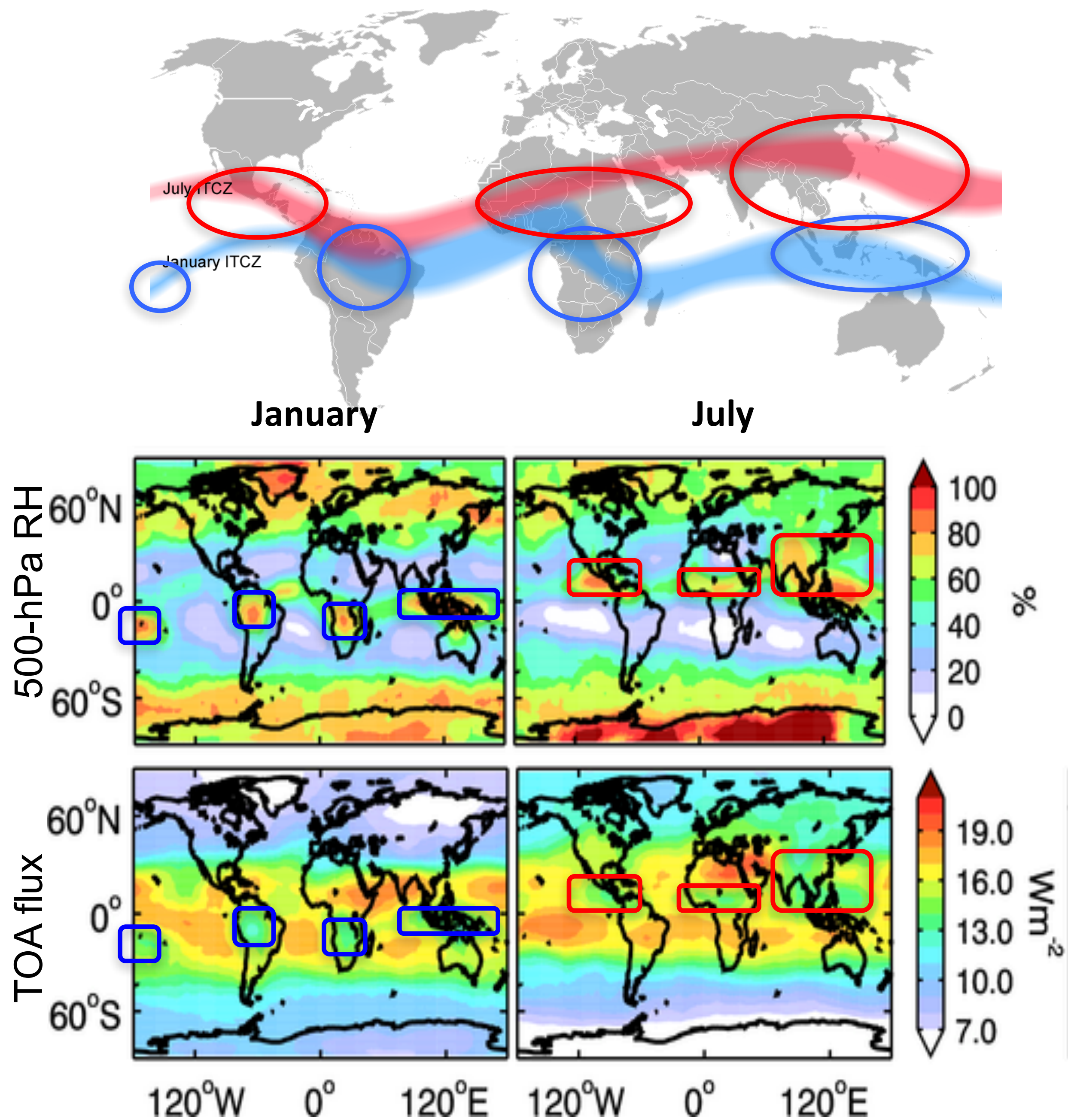

ITCZ shift from south of equator to north of equator from January to July.

- **Inside ITCZ belt:**
  - **Deep convection**
  - **Wet, rainy season, and cloudy sky**
- **Outside ITCZ belt:**
  - **Subsidence region**
  - **Arid and clear sky**
- **January: deep convection zone at central Pacific, Amazon, S. Africa (Congo basin), and Indonesia.**
- **July: deep convection zone occur north of equator at E. Tropical Pacific, Africa Savanna, southeast Asia.**

Relative Humidity (RH)

The amount of water vapor present in air expressed as a percentage of the amount needed for saturation at the same temperature.

The ratio of the partial pressure of water vapor in the mixture to the equilibrium vapor pressure of water at a given temperature.

$$RH = \frac{e_w(H_2O,P)}{e_w^*(T,P)}$$

$$e_w^*(T,P) = (1.0007 + 3.46 \times 10^{-6} P) \times (6.1121) e^{\left(\frac{17.502T}{240.97+T}\right)}$$

RH describes the state of atmospheric saturation and suggests the cloud distribution based on the combination of water vapor and temperature.